RSC Advances

Structures and Third-Order Nonlinear Optical Properties of TwoThree-dimensional Cd(II) Coordination Polymers with trinodal (3, 4, 5) and dinodal (4, 5) connected network topologies

Journal:	*RSC Advances*
Manuscript ID	RA-ART-07-2015-014734.R3
Article Type:	Paper
Date Submitted by the Author:	15-Sep-2015
Complete List of Authors:	lian, zhaoxun; Henan Normal University, School of Chemistry and Chemical Engineering; Henan Institute of Science and Technology, Postdoctoral Research Base Jiang, Kai; Henan Normal University, School of Chemistry and Chemical Engineering Lou, Tianjun; Henan Institute of Science and Technology, Postdoctoral Research Base
Subject area & keyword:	

RSC Advances

ARTICLE

Structures and Third-Order Nonlinear Optical Properties of TwoThree-dimensional Cd(II) Coordination Polymers with trinodal (3, 4, 5) and dinodal (4, 5) connected network topologies

Received 00th January 20xx,
Accepted 00th January 20xx

DOI: 10.1039/x0xx00000x

www.rsc.org/

Zhaoxun Lian[ab], Kai Jiang*[a],Tianjun Lou[b]

Two Cd(II) coordination polymers, $[Cd_3(1, 2\text{-bib})_4(STP)_2(H_2O)_2]\cdot 10H_2O$ (**1**) and $[Cd_3(1, 3\text{-bib})_5(STP)_2]\cdot 3H_2O$ (**2**) (1, 2-bib = 1, 2-bis(imidazol-l-yl-methyl)benzene; 1, 3-bib = 1, 3-bis(imidazol-l-yl-methyl)benzene; NaH_2STP = sodium 3,5-dicarboxybenzenesulfonate), have been synthesized under hydrothermal conditions. Compound **1** presents a 3-nodal (3, 4, 5)-connected 3D framework with a point (Schläfli) symbol $(4.6^2)_2(4^2.6^4.8^4)_2(4^2.8^4)$. Compound **2** exhibits a 3D framework with 2-nodal(4, 5)-connected $(4^2.5^3.6^5)_2(5^2.6^4)$ topology. The third-order nonlinear optical (NLO) properties of two compounds were determined in DMSO solution and thin films by Z-scan technique. They show strong third-order nonlinear optical (NLO) absorption with absorptive coefficients β(MKS) 6.53×10^{-11} m·W^{-1} for **1** and 7.15×10^{-11}m·W^{-1} for **2** in DMSO solution. The third-order NLO susceptibility $\chi^{(3)}$ are calculated as 2.23×10^{-12} for **1**, 2.50×10^{-12} *esu* for **2** in DMSO solution. While in thin films, both compounds show quite stronger NLO absorption with absorptive coefficients β(MKS) 31.1×10^{-6} m·W^{-1} for **1** and 3.80×10^{-6} m·W^{-1} for **2**, and third-order NLO susceptibility $\chi^{(3)}$ are calculated as 1.09×10^{-6} for **1**, 0.13×10^{-6} *esu* for **2**. The electronic structures of two compounds were investigated by density functional theory (DFT). The composition of frontier orbitals and the origin of the NLO properties of two compounds were discussed.

1. Introduction

With the development of economy and society, there are increasing demands for the third-order nonlinear (NLO) materials, owing to applications of these materials in optical fibers, data storage, optoelectronic devices, high speed optical communication networks and display technologies[1-5]. For this reason many inorganic semiconductors, conjugated polymers, Organic materials and clusters compounds Mo(W)/S/M (M = Cu, Ag, Au, Pt, Pd, Fe, Co, etc.) have been reported[6-12]. Previous studies showed that porphyrin and its analogues exhibit excellent third-order optical nonlinearity owing to their extended π-conjugated structure[13-17]. By introducing different groups or metal ions, the third order nonlinear optical properties of porphyrin and its analogues can be tuned. Heterometallic clusters Mo(W)/S/M (M = Cu, Ag, Au, Pt, Pd, Fe, Co, etc.) with extensive dπ-pπ delocalized systems and dπ-dπ conjugated systems, derived from tetrathiometallate $[MS_4]^{2-}$ (M = Mo, W) anions showed good third-order NLO effects, and appeared to be ideal candidate for third-order NLO materials[12]. Zhang and Lang have reported a few of heterometallic clusters Mo(W)/S/M [12,18-20]. Their works showed that the structural units, peripheral ligands, skeleton elements and constructing components have considerable influence on the NLO functions of materials. The enhancement of the NLO performances of the heterometallic clusters Mo(W)/S/M can possibly be tuned through structural manipulation. Metal-organic coordination polymers (CPs) combine the advantages of organic and inorganic species, and exhibit variety of excellent properties, including luminescence, catalysis, molecular adsorption, and molecular sensing[21-24]. The CPs have greater design flexibility via varying the center metals, ligands, coordination geometry, and oxidation state. Further, the charge-transfer nature of the metal-ligand bonds enhances the nonlinearity. However, the study of the third-order NLO properties of the CPs is little. Hou and his coworkers reported a few of coordination polymers constructed from pyridine, imidazole and their derivatives. They used Z-scan technique to investigate third-order NLO properties of these compounds in solution[25-33]. These materials exhibit a variety of third-order nonlinearities. Some of them showed excellent optical-limiting (OL) performance[33]. These excellent works continue to inspire us to explore the NLO properties of CPs. In this paper, we selected 1, 2-bib and 1, 3-bib and STP as spacers to synthesize coordination polymers via self-assembly reactions. The 1, 2-bib and the 1, 3-bib ligand bearing a-(CH_2)- spacer are semirigid. Their two imidazolyl groups can rotate on the -(CH_2)- group to accommodate the

[a] School of Chemistry and Chemical Engineering, Henan Normal University, Xinxiang 453007, People's Republic of China. Email: zhxalian@163.com.
[b] Postdoctoral Research Base, Henan Institute of Science and Technology, Xinxiang 453003, People's Republic of China.

Electronic Supplementary Information (ESI) available: [details of any supplementary information available should be included here]. See DOI: 10.1039/x0xx00000x

coordination geometries of the central metal atoms in various coordination conformations[34-37]. The STP ligand is a highly symmetrical carboxylate one, and has been widely used to construct coordination polymers[38,39]. The combination of 1, 2-bib and 1, 3-bib ligands and STP ligands is a feasible strategy to construct CPs. Two Cd(II) coordination polymers were obtained. The Z-scan technique was employed to investigate NLO performance of two compounds in thin films and DMSO solution.The electronic structures of two compounds were investigated by density functional theory (DFT)[40]. The results show that the composition of frontier orbitals plays an important role on the NLO properties of two compounds.

2. Experimental

2.1 Materials and measurements

All chemical materials were A. R. Grade, and used as received. The ligand 1, 2-bib and the 1, 3-bib were prepared by methods reported previously[36]. Elemental analyses for carbon, hydrogen and nitrogen were carried out with an Elementary Vario MICRO elemental analyzer. The FT-IR spectra were recorded within the 400 ~ 4000cm^{-1} region on a Perkin-Elmer spectrum-2000 with KBr pellets. Electronic spectra were measured on a shimadzu UV-3100 spectrophotometer.

2.2 Synthesis of [Cd_3(1, 2-bib)$_4$(STP)$_2$(H_2O)$_2$]·10H_2O (1)

A mixture of $Cd(CH_3COO)_2{\cdot}4H_2O$ (0.1mmol, 0.028g), NaH_2STP(0.2mmol, 0.028g) and 1, 2-bib (0.2mmol, 0.047g) in distilled water (10mL), with the pH value adjusted to 5.0 by the addition of 0.2M NaOH, was transferred into a Parr Teflon-lined stainless steel vessel, and then sealed and heated to 413K for 3 days, followed by cooling to ambient temperature spontaneously. Colorless block-like crystals were collected by hand, washed with distilled water and dried in air at ambient temperature. Yield 81% based on Cd. *[Cd_3(1, 2-bib)$_4$(STP)$_2$(H_2O)$_2$]·10H_2O* **1** Elemental anal. calcd for **1**: C,43.39; N, 11.25; H, 4.35%. Found: C, 43.37; N,11.26; H, 4.36%. FT-IR(KBr): ν_{max} 3434, 3141, 1608, 1562, 1511, 1434, 1375, 1232, 1110, 1085, 1054, 929, 838, 784, 752, 723 and 659 cm^{-1}.

2.3 Synthesis of [Cd_3(1, 3-bib)$_5$(STP)$_2$]·3H_2O (2)

The synthesis of compound **2** was similar to the above description for compound **1** except that 1, 3-bib(0.2mmol, 0.047g) was used instead of 1, 2-bib. [Cd_3(1, 3-bib)$_5$(STP)$_2$]·3H_2O **2**, yield 69% based on Cd, Elemental anal. calcd for **2**: C, 49.97; N, 13.55; H, 3.90%. Found: C, 49.96; N, 13.57; H, 3.88%. FT-IR(KBr): ν_{max} 3446, 3124, 1610, 1567, 1525, 1442, 1386, 1283, 1093, 952, 835, 755, 723 and 655 cm^{-1}.

2.4 Crystal structure determination

The X-ray intensity data for two compounds were recorded on a Bruker Smart CCD using Mo Kα radiation and a graphite monochromator at room temperature. The diffraction data was integrated by using the SAINT program. Multi-scanabsorption corrections were applied using the SADABS program. All heavy atoms were found by direct methods with SHELX-97[41]; other non-hydrogen atoms were found by difference Fourier synthesis. All non-hydrogen atoms were refined with anisotropic displacement parameters by the full-matrix least-squares refinement. Hydrogen atoms bound to C atoms were placed geometrically and held in the rigid mode.The lattice water molecules in **1** are disordered. The 1, 3-bib ligand in **2** is disordered by symmetry. Crystal data and structural refinement of the structures are summarized in Table 1. Selected bond lengths and angles are presented in Tables 2.

Table 1 Crystallographic data for compound **1** and **2**.

	Compound **1**	Compound **2**
Formula	$C_{72}H_{86}Cd_3N_{16}O26S_2$	$C_{86}H_{80}Cd_3N_{20}O_{17}S_2$
M_r	1992.89	2067.02
T(K)	293(2)	293(2)
Crystal system	Monoclinic	Monoclinic
Space group	*$P2_1/c$*	*C2/c*
a(Å)	10.6010(2)	37.955(1)
b(Å)	17.872(3)	10.455(5)
c(Å)	21.185(4)	24.091(5)
α(˚)	90	90
β(˚)	96.196(3)	109.550(5)
γ(˚)	90	90
V(Å^3)	3990.4(1)	9009(5)
Z	2	4
$D_{calc.}$(g/cm^3)	1.659	1.524
F(000)	2028	4192
Abs-coeff (mm^{-1})	0.934	0.825
Reflections collected	27258	27802
Unique reflections	9224	10960
Data/restraints/para	9224 / 15/ 558	10960 / 0 / 518
Goof on F^2	1.039	1.059
R_1, wR_2 [I>2σ(I)]	0.0411, 0.0909	0.0729, 0.1934
R_1, wR_2 (all data)	0.0660, 0.1152	0.117, 0.2213

Table 2 Selected bond length (Å) and bond angles(º) for compound **1** and **2**.

Compound **1**			
Cd(1)-N(1)	2.279(4)	Cd(1)-N(8)a	2.283(4)
Cd(1)-O(1)	2.317(3)	Cd(1)-O(4)b	2.359(3)
Cd(2)-N(4)	2.212(4)	Cd(2)-O(8)	2.333(3)
Cd(2)-O(5)a	2.408(3)	Cd(2)-O(5)d	2.408(3)
Cd(1)-N(5)	2.284(4)	Cd(2)-N(4)c	2.212(4)
Cd(2)-O(8)c	2.333(3)		
N(1)-Cd(1)-N(8)a	90.50(1)	N(1)-Cd(1)-N(5)	92.17(1)
N(1)-Cd(1)-O(1)	130.46(1)	N(8)a-Cd(1)-O(1)	88.67(1),
N(8)a-Cd(1)-N(5)	175.48(1)	N(5)-Cd(1)-O(1)	86.82(1)
N(1)-Cd(1)-O(4)b	132.57(1)	N(8)-Cd(1)-O(4)b	91.18(1)
O(1)-Cd(1)-O(4)b	96.97(1)	N(4)c-Cd(2)-O(8)	88.53(1)
N(5)-Cd(1)-O(4)b	89.71(1)	N(4)-Cd(2)-O(8)	91.47(13)
N(4)-Cd(2)-O(8)c	91.47(1)	N(4)-Cd(2)-O(8)c	88.53(1)
N(4)c-Cd(2)-O(5)a	92.56(1)	O(8)c-Cd(2)-O(5)a	83.39(1)
O(8)-Cd(2)-O(5)d	83.39(1)	N(4)-Cd(2)-O(5)d	92.56(1)
N(4)-Cd(2)-O(5)a	87.44(1)	O(8)-Cd(2)-O(5)a	96.61(1)
N(4)-Cd(2)-O(5)d	87.44(1)		
Compound **2**			
Cd(1)-O(2)	2.254(3)	Cd(1)-N(9)	2.310(4)
Cd(1)-N(1)	2.379(4)	Cd(1)-O(4)a	2.400(3)
Cd(1)-N(5)	2.372(4)	Cd(1)-O(3)a	2.538(4)
Cd(2)-N(4)	2.302(6)	Cd(2)-N(4)d	2.302(6)
Cd(2)-N(8)b	2.201(5)	Cd(2)-N(8)c	2.201(5)
O(2)-Cd(1)-N(9)	129.82(1)	O(2)-Cd(1)-N(5)	96.01(13)
O(2)-Cd(1)-N(1)	87.59(1)	N(9)-Cd(1)-N(1)	86.39(15)
N(9)-Cd(1)-N(5)	90.02(1)	N(5)-Cd(1)-N(1)	176.03(1)
N(8)c-Cd(2)-N(4)	103.3(2)	N(8)b-Cd(2)-N(8)c	147.3(2)
O(2)-Cd(1)-O(4)a	93.02(3)	N(8)b-Cd(2)-N(4)	99.8(2)
N(4)-Cd(2)-N(4)d	89.2(3)	O(4)a-Cd(1)-O(3)a	53.12(1)
N(8)b-Cd(2)-N(4)	99.8(2)	N(8)c-Cd(2)-N(4)	103.3(2)

Symmetry code: for 1.a, x,-y+3/2,z+1/2; b, x-1,y,z; c, 3 -x+1,-y+1,-z+2; d, -x+1,y-1/2,-z+3/2.for 2. a, x,y+1,z ; b, x+1/2,y+1/2,z+1; c, -x+1/2,y+1/2,-z+1/2; d, -x+1,y,-z+3/2.

2.5 Nonlinear optical measurements

The DMSO solutions of **1** and **2** were placed in a 1mm quartz cell for NLO measurements.To prepare the CPs thin films, the powders of CPs were dispersed into ethanol with ultrasonic processing. Then the mixed solution was spin-coated (1500rpm, 20s) onto the cleaned quartz glass substrates and dried at room temperature for 24h. The thickness of the film was measured by a thickness gauge (about 3μm for **1** and 5μm for **2**). The nonlinear optical refraction and absorption were obtained with a linearly polarized laser light (7ns, 10Hz, 532nm) generated from mode-locked Q-switched Nd:YAG laser. The spatial profiles of the optical pulses are nearly Gaussian after passing through a filter. The focal length of the positive lens is 30 cm. Incident and transmitted pulsed energies are measured simultaneously by two energy detectors (RJP-765 Energy probes, laser precision, Laserprobe Corp), which are linked to a computer through an RS232 interface. The sample was mounted on a translation stage that was controlled by the computer to move along the z-axis with respect to the focal point. An aperture 0.5 mm radius was placed in front of the transmission detector, and the transmittance was recorded as function of the sample position on the Z-axis (closed aperture Z-scan). For measuring the NLO absorption, the Z-dependent sample transmittance was taken without the aperture (open aperture Z-scan). In our experiments, we preformed a Z-scan on the solvent (DMSO) at the pulse energy focused on our samples, and no obvious nonlinear optical phenomenon was observed.

3. Results and discussion

3.1 Structure of 1

Selected bond distances and angles are listed in Table 2. Structural analysis reveals that the compound **1** exhibits a complicated three-dimensional structure. Complex **1** crystallizes in the monoclinic system, $P2_1/c$ space group. The asymmetric unit contains two crystallographically independent cadmium (II) ions, as shown in Figure 1(a). The Cd1 is coordinated by two oxygen atoms from two different STP ligands and three nitrogen atoms from three 1,2-bib ligands, to exhibit a triangular pyramid geometry. The Cd-N and Cd-O lengths are 2.279(4) and 2.359(3) Å, respectively, which are both within the ranges reported for Cd(II) complexes[38]. The Cd2 is located on a symmetry center, and six-coordinated by four oxygen atoms from two sulfonate group of two STP ligands and two aqua ligands, and two nitrogen atoms from two 1, 2-bib ligands, to display a distorted octahedral geometry. The Cd-N and Cd-O lengths range from 2.212(4) and 2.408(3) Å. There is a unique STP ligand in the asymmetric unit, which is tridendate. Each carboxylate group of STP and the sulfonate group are coordinated to Cd(II) in monodendate mode. The whole STP ligand adopts μ_3-η^1: η^1: η^1 coordination mode. The 1, 2-bib ligand links two Cd(II) in a cis conformation.

In **1**, STP ligands act as μ_3-bridges to assemble Cd(II) ions into ladder-like chains along the a axis, as shown in Figure

1(b). Interaction of Cd(II) ions through bridging 1, 2-bib ligands results in two dimensional grid sheets, as shown in Figure 1(c). These chains and the sheets are further connected by 1, 2-bib ligands via adjacent Cd(ii) ions to form a complicated three-dimensional structure. In comparable structure[42], the 1, 2-bib ligands act as pillars to bridge the adjacent [Co_2(butca)] layers to afford a porous 3D host frameworks with two kinds of metal-1, 2-bib helical chains. In other related compounds[43, 44], the flexible bis(imidazole) ligands assemble transition metal ions into 1D, 2D and 3D structures, respectively. In Zn(II) complex[38], the 1, 2-bib ligands and carboxylate ligands coordinate to Zn(II) centers to a twofold interpenetration of nets. To further understand the structure of **1**, topological analysis by reducing multidimensional structure to simple node-and linker net was performed. Pentacoordinate Cd1 and hexacoordinate Cd2 can be viewed as a five-connector and four-connector, respectively. Each 1, 2-bib and STP ligand in turn connects two and three Cd(II) ions, respectively, hence can be regarded as two and three-connector. The analysis of the topology was carried out by using the TOPOS (V4.0) program. The result shows that the structure of **1** is a (3, 4, 5)-3-nodal three dimensional net with a point (Schläfli) symbol (4.6^2)$_2$(4^2.6^4.8^4)$_2$(4^2.8^4), as shown in Figure 1(d).

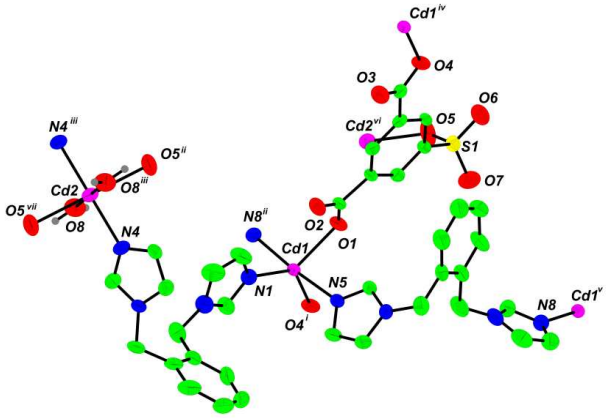

Figure 1(a). View of **1** showing the local coordination environment of Cd(II) ion. Thermal ellipsoids are drawn at 50% probability. Hydrongen atoms are omitted for clarity. Symmetry code; i: -1+x, y, z;ii: x, 1.5-y, 0.5+z;iii: 1-x, 1-y, 2-z;iv: 1+x, y, z;v: x, 1.5-y, -0.5+z; vi: 1-x, 0.5+y, 1.5-z;vii: 1-x, -0.5+y, 1.5-z.

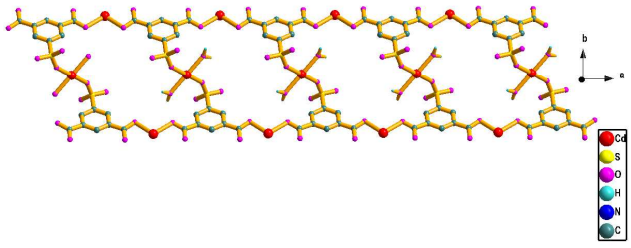

Figure 1(b). The ladder-like chain structure constructed by STP and Cd(II) in **1**

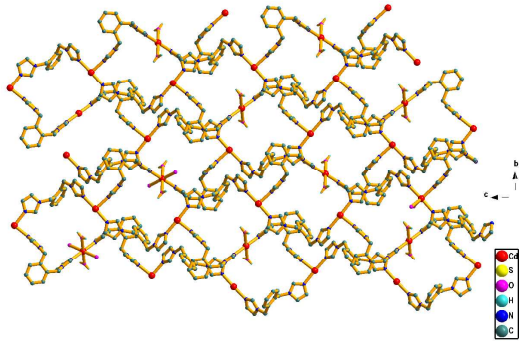

Figure 1(c). 2D-sheet structure constructed by 1,2-bib and Cd(II) in **1**

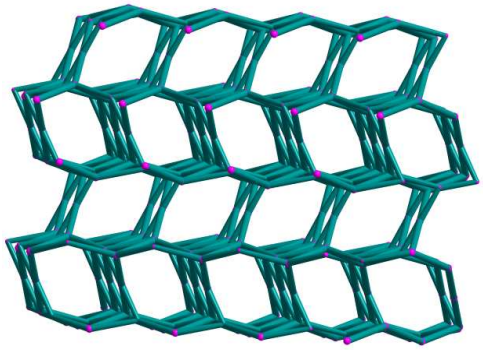

Figure 1(d). Schematic representation of 3-nodal (3, 4, 5)-connected 3D framework of **1**.

3.2 Structure of 2

When 1, 3-bib ligand was used instead of 1, 2-bib, the compound **2** was obtained. X-ray crystallographic analysis reveals that **2** crystalllizes in monoclinic space group C2/c. There are two independent cadmium(ii) ions, one STP anion and two and half 1,3-bib ligands in the asymmetric unit, as shown in Figure 2(a). The 1, 3-bib ligand containing N9 atom is disordered over two sites with occupancies of 0.50 and 0.50 by symmetry. Cd1 ion is coordinated by three oxygen atoms from two carboylic groups of two different STP ligands, and three nitrogen atoms from three 1, 3-bib molecules. The coordination geometry for the Cd1 atom can be described as a distorted octahedron. The Cd-N and Cd-O distances are in the range 2.254(3) to 2.538(4) Å. These distances fall in the normal range found in other cadmium complexes[38]. Cd2 is located on the crystallographic inversion center, and four-coordinated to complete tetrahedral coordination geometry. The four donors coordinated to Cd2 come from four imidazolyl nitrogen atoms from four 1, 3-bib ligands. The Cd-N bond lengths range between 2.201(5)-2.302(6) Å. The closest separation of Cd2 and O7 is much longer than other ones, which suggests a weak non-covalent interaction. The independent STP ligand is bidentate. Each carboxylate group coordinates to Cd(II) center in monodentate mode, while the sulfonate group does not participate in coordination. The whole STP ligand acts as a μ_2-η^1: η^1 bridge to connect two Cd(II) centers.

In **2**, Interaction of Cd(II) ions and STP ligands results in an infinite chain, as shown in Figure 2(b). Adjacent chains are linked by 1, 3-bib ligands via adjacent Cd(ii) ions to form a complicated three-dimensional structure, as shown in Figure 2(c). In comparable structure[45], the 1, 3-bib ligand adopts the syn conformation, with both imidazole groups on the same side of the central benzene ring. The metal ions infinitely connected by 1, 3-bib and dicarboxylate ligands to generate a 1D loop-like chain. In related nickel(II) complex, the 1, 3-bib adopts an anti-conformation. The neighboring $[Ni_2(ip)_2]$ ladder chains are further cross-linked by 1,3-bib ligands to construct a complicated 3D framework with the point symbol of $\{4^2.6^5.8^3\}\{4^2.6\}$. The network topology of **2** is further analyzed. The Cd1 center is six-connected with vertex symbol of $\{4^2.5^3.6^5\}$, and Cd2 is four connected with vertex symbol of $\{5^2.6^4\}$. Obviously, the STP ligand and 1,3-bib ligand are only a 2-connected spacer. As a result, a complicated 3D 2-nodal coordination framework with (4, 5) connectivity is formed, which has the Schläfli symbol of $\{4^2.5^3.6^5\}_2\{5^2.6^4\}$, as shown in Figure 2(d).

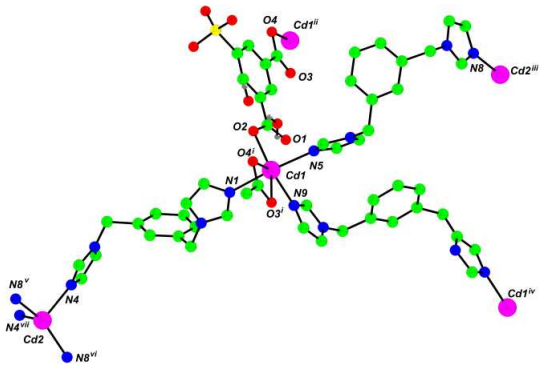

Figure 2(a).View of **2** showing the local coordination environment of Cd(II) ion. Thermal ellipsoids are drawn at 50% probability. Hydrongen atoms are omitted for clarity. Symmetry code; i: x, 1+y, z;ii: x, -1+y, z;iii: -0.5+x, -0.5+y, -1+z;iv: 0.5-x, 0.5-y, -z;v: 0.5+x, 0.5+y, 1+z;vi: 0.5-x, 0.5+y, 0.5-z;vii: 1-x, y, 1.5-z.

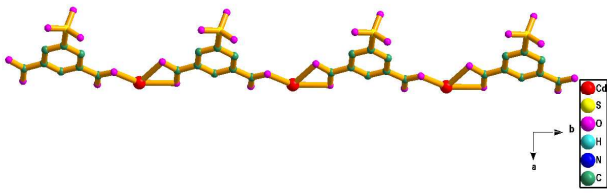

Figure 2(b). The chain structure constructed by STP and Cd(II) in **2.**

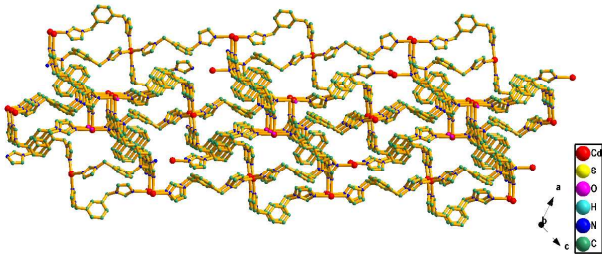

Figure 2(c). The 3D structure constructed by 1,3-bib and Cd(II) in **2.**

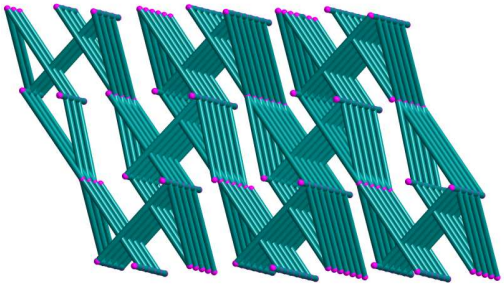

Figure 2(d). Schematic representation of 2-nodal (4, 5)-connected 3D framework of **2**.

3.3 PXRD and thermal analysis

In order to check the phase purity of these compounds, the X-ray power diffraction (XRPD) patterns of compounds 1 and 2 were checked at room temperature. The results show that the peak positions of the simulated and experimental patterns are in agreement with each other, indicating the good phase purity of the compounds.

The thermal gravimetric analyses of 1 and 2 were carried out. The results show that the TGA curves of 1 and 2 exhibit an initial weight loss from room temperature to 150°C, with the observed weight loss of 10.5% for 1 and 10.1% for 2 corresponding to the release of coordinated and lattice water molecules. For 1, the decomposition of the anhydrous composition occurs in the temperature range of 245-430, corresponding to the loss of 1, 2-bib ligands. The frameworks of 2 are stable up to 286, and begin to decompose upon further heating.

3.4 Linear and Nonlinear optical properties

Two compounds exhibit similar electronic absorption spectra. Absorption peaks were observed at < 300nm. Two compounds have relatively low linear absorption in the visible and near-IR regions. Wavelength of laser in our experiment is 532nm, which can not cause resonance absorption.

The NLO properties of **1** and **2** were investigated with a pulse width of 7ns at 532nm and 10Hz repetition rate. The Figure 3 depicts the nonlinear absorptive properties of **1** and **2**. The following formulas (1) and (2) are used to calculate the nonlinearabsorptive coefficient,

$$T(z)=\frac{1}{\sqrt{\pi}q(z)}\int_{-\infty}^{\infty}\ln[(1+q(z)]e^{-\tau^2}d\tau \quad (1)$$

$$q(z)=\beta I(z)\frac{1-e^{-\alpha_0 L}}{\alpha_0} \quad (2)$$

which describe a third-order NLO process[46, 47]. T(z) represents the transmittance, defined as the ratio of the transmitted pulse energy and incident pulse energy. τ is pulse length. α_0 and β are the linear and nonlinear absorption coefficients, respectively. L is the sample thickness. I_0 is the peak irradiation intensity at focus. From

Figure 3, the open aperture data clearly suggest the presence of reverse saturable absorption (RSA) type behavior. The NLO absorption of **1** and **2** increases as the incident light irradiance rises since light transmittance (T) is a function of the sample's Z position. The closer the focus, the lower the transmittance. The normalized transmittance drops to about 0.67 for **1**, and 0.26 for **2** at the focus, respectively. The corresponding third-order NLO absorptive coefficient β(MKS) are 6.53×10^{-11} m·W^{-1} for **1** and 7.15×10^{-11}m·W^{-1} for **2** in DMSO solution. The β values of **1** and **2** are comparable with that those of some clusters and CPs[12, 26-33]. The corresponding third-order NLO susceptibility $\chi^{(3)}$ are calculated as 2.23×10^{-12} for **1**, 2.50×10^{-12} *esu* for **2** in DMSO solution. Although a few of well performing third-order NLO CPs have been reported, the NLO data obtained was from solution state[26-33]. These data often contained aspects of the solvent and the materials. This is not the NLO performance of neat materials. In our experiment, we have prepared the thin film of two compounds by conventional spin coating method, and evaluated the NLO component of two compounds. Figure 4 presents the open aperture data of **1** and **2**. The normalized transmittance drops to about 0.34 for **1**, and 0.78 for **2** at the focus. Two compounds show much stronger absorption in solid state with third-order NLO absorptive coefficient β(MKS) 31.1×10^{-6} m·W^{-1} for **1** and 3.80×10^{-6} m·W^{-1} for **2**. The third-order NLO susceptibility $\chi^{(3)}$ are calculated as 1.09×10^{-6} for **1**, 0.13×10^{-6} *esu* for **2**. Owing to lack of the third-order NLO susceptibility $\chi^{(3)}$ of neat CPs, we cannot carry out comparative analysis, but the $\chi^{(3)}$ values of **1** and **2** in solid state are much larger than those of other neat materials, such as neat inorganic semiconductors (about 10^{-10}*esu*) and conjugated polymers[48,49].

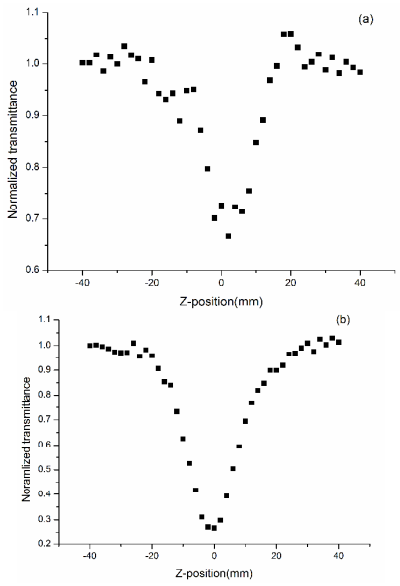

Figure 3 (a) and (b). NLO absorptive properties of compound **1** and **2** in DMSO solution.

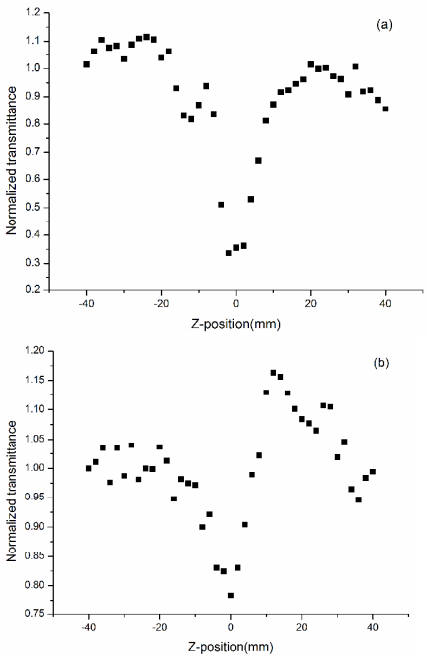

Figure 4(a) and (b). NLO absorptive properties of compound **1**and **2** in thin films.

3.4 DFT calculation

Previous studies showed that the NLO properties of π-conjugated systems originate from the delocalization of the π-electron cloud, which corresponds to the frontier orbitals. Energy gap between the HOMO and LUMO also has a great influence on the NLO of materials[50-52]. A narrower band gap leads to larger optical nonlinearity, whereas a wider band gap yields better LDT (laser-damage threshold). Yet, high NLO susceptibility and LDT are not mutually exclusive. Hence, analysis of the composition of the frontier orbitals and energy gap can be an effective way to understand the origin of the NLO performance. In the present work, both compound **1** and **2** contain two independent cadmium(ii) ions. We selected {Cd(1, 2-bib)$_3$(phCOO)$_2$} and {Cd(1, 2-bib)$_2$(H_2O)$_2$($phSO_3$)$_2$} for compound **1**, {Cd(1, 3-bib)$_3$(phCOO)$_2$} and {Cd(1, 3-bib)$_4$ ($phSO_3$)$_2$} for compound **2** as computing units, and calculated the frontier obitals of these units by density functional theory (DFT) based 6-31G basis set for C, H, N, O, and S and LanL2DZ for cadmium. The composition of the frontier orbitals was calculated by using Multiwfn software packages[53]. The calculation results are listed in the Table 3. It can be seen that the composition of the frontier orbitals of two compounds mainly contain contributions of imidazolyl groups, phenyl groups and carboxyl groups. These the frontier orbitals have barely any Cd(II) centers character. For compound **1**, HOMO is primarily carboxyl groups and imidazolyl groups-based orbitals, and LUMO is primarily imidazolyl group and phenyl group-based orbitals. Similar cases are found in compound **2**, but contributions of imidazolyl groups, phenyl groups and carboxyl groups in **2** are larger than those of **1**. In general,

delocalization of the π-electrons in HOMO to LUMO will be the first excited singlet state S_1 or the first excited triplet state T_1. The photochemical and photophysical properties of materials are controlled by the first excited singlet state S_1 or the first excited triplet state T_1. Figure 5 and 6 depict the composition of the frontier orbitals of **1**. Two Figures clearly show two types of potential delocalization of the electron cloud. One kind is from carboxyl group to phenyl group of 1, 2-bib. The other kind is from imidazolyl group to phenyl group of 1, 2-bib, which corresponds to intra-molecular charge transfer. Figure 7 and 8 depict the composition of the frontier orbitals of **2**. In the case of $\{Cd(1,3\text{-bib})_3(phCOO)_2\}$, the potential delocalization of the electrons is similar to that found in **1**, while in $\{Cd(1,2\text{-bib})_4\ (phSO_3)_2\}$, potential delocalization of the π-electrons happens between the imidazolyl group to another phenyl group of 1, 2-bib corresponding to intermolecular charge transfer. The calculation results show the delocalization of π-electrons in **1** will be easier than that of **2**, which can enhance the susceptibility of the molecules. Two compounds show almost the same third-order NLO susceptibility $\chi^{(3)}$ (2.23×10^{-12} for **1**, 2.50×10^{-12} *esu* for **2**) in DMSO solution. This may be that solvent effect weakens the difference of potential delocalization of the π-electrons in polar solvent DMSO. In order to reveal the NLO performance of neat materials, we evaluated the NLO component of two compounds in thin films. The open aperture data presented that the third-order NLO susceptibility $\chi^{(3)}$ of compound **1** is 8 times that of **2** (1.09×10^{-6} for **1**, 0.13×10^{-6} for **2**). This result is in line with our expectations and in agreement with the calculation results. The photon energy of the laser in our experiment (2.33ev) is about 1/2 of the energy gap between the LUMO and the HOMO. Experimental and calculation results show that the NLO of two compounds are governed by the excited state absorption and two photon absorption.

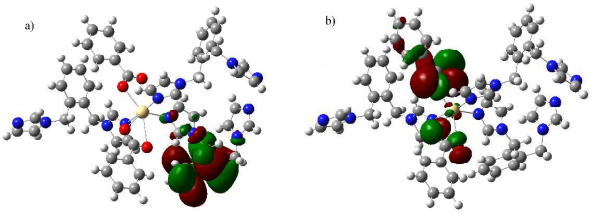

Figure 5. The frontier orbital of $\{Cd(1,2\text{-bib})_3(phCOO)_2\}$: (a) LUMO, (b) HOMO. Cd yellow, N blue, O red, C gray, H white.

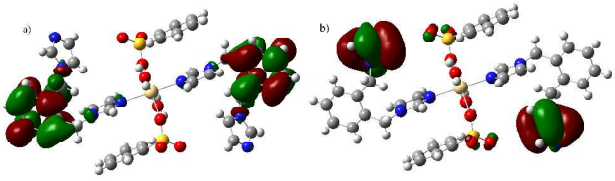

Figure 6. The frontier orbital of$\{Cd(1,2\text{-bib})_2(H2O)_2(phSO_3)_2\}$: (a) LUMO, (b) HOMO. Cd yellow, N blue, O red, C gray, H white.

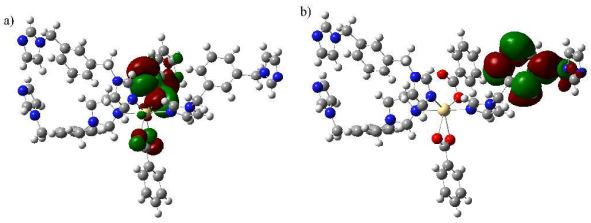

Figure 7. The frontier orbital of $\{Cd(1,3\text{-bib})_3(phCOO)_2\}$: (a) LUMO, (b) HOMO. Cd yellow, N blue, O red, C gray, H white.

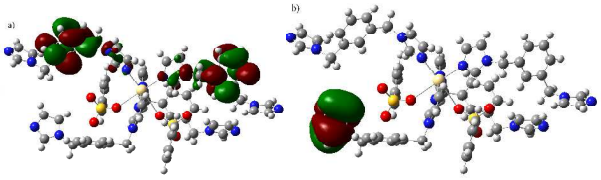

Figure 8. The frontier orbital of $\{Cd(1,2\text{-bib})_4\ (phSO_3)_2\}$: (a) LUMO, (b) HOMO. Cd yellow, N blue, O red, C gray, H white.

Table 3.The composition and the energy gap of the frontier orbitals of **1** and **2** (%, eV)

Compound 1				
	Cd1		Cd2	
	LUMO	HOMO	LUMO	HOMO
Imidazolyl group	14.64	-	14.19	91.11
Phenyl group	67.98	7.21	64.33	-
Carboxyl group	-	87.55	-	-
energy gap	4.53		5.07	
Compound 2				
	Cd1		Cd2	
	LUMO	HOMO	LUMO	HOMO
Imidazolyl group	10.26	-	18.04	95.77
Phenyl group	75.29	7.98	62.54	
Carboxyl group		87.41	-	
energy gap	4.62		4.65	

Conclusions

In summary, by reactions of cadmium(II) acetate with STP ligands and 1, 2-bib and 1, 3-bib ligands, two 3D-CPs with trinodal and dinodal connected networks topologies were obtained. Two compounds show excellent NLO performance in solution and thin films. Especially, two compounds exhibit very strong NLO absorption in thin films. The value of susceptibility $\chi^{(3)}$ are much larger than those of other neat inorganic semiconductors (about 10^{-10}*esu*), conjugated

polymers. Two compounds appeared to be ideal candidate for third-order NLO materials. The composition of the frontier orbitals of two compounds was calculated by DFT. We induce that the NLO performance of two compounds is governed by STP ligands and/or 1, 2-bib ligands, 1, 3-bib ligands.

Acknowledgements

We gratefully acknowledge the financial support by Post Doctoral Fund of Henan Institute of Science and Technology.

Supplementary material

CCDC (1423082-1423083) contains the supplementary crystallographic data for **1** and **2**. These data can be obtained free of charge via http://www.ccdc.cam.ac.uk/conts/retrieving. html, or from the Cambridge Crystallographic Data Centre, 12 Union Road, Cambridge CB2 1EZ, UK; fax: (+44) 1223-336-033; or e-mail: deposit@ccdc.cam.ac.uk.

References

1. G. S. He, L. Tan, Q. Zhang, and P. N. Prasad, *Chem. Rev*, 2008, 108, 1245.
2. D. M. Burland, R. D. Miller and C. A. Walsh, *Chem. Rev*, 1994, 94, 31.
3. J. Zyss, Molecular Nonlinear Optics: Materials, Physics and Devices; Academic Press, Boston, MA, 1994.
4. C. Bosshard, K. Sutter, P. Prêtre, J. Hulliger, M. Flörsheimer, P. Kaatz, P. Günter, Organic Nonlinear Optical Materials; Gordon and Breach, Amsterdam, Netherlands, 1995.
5. J. L. Brédas, C. Adant, P. Tackx, A. Persoons, B. M. Pierce, *Chem. Rev*, 1994, 94, 243.
6. P. Gaur, B. P. Malik, D. Sharma and A. Gaur, *NANO*, 2015, 10, 1.
7. N. R. Evans, L. S. Devi,C. S. K. Mak, S. E. Watkins, S. I. Pascu, A. Kohler, *J. Am. Chem Soc*, 2006, 128, 6647.
8. P. Dutta, H. Park, W. H. Lee, I. N. Kang, S. H. Lee, *Polym. Chem*, 2014, 5, 132.
9. Q. Hou, J. Liu, T. Jia, S. Luo, G. Shi, *J. Appl. Polym. Sci*, 2013, 130, 3276.
10. W. Zhuang, M, Bolognesi, M. Seri, P. Henriksson, D. Gedefaw, R. Kroon, *Macromolecules*, 2013, 46, 8488.
11. P. M. Beaujuge, J. R. Reynolds, *Chem. Rev*, 2010, 110, 268.
12. C. Zhang, Y. L. Song, X. Wang, *Coord. Chem. Rev*, 2007, 251, 111.
13. K. J. Thorley, J. M. Hales, H. L. Anderson, and J. W. Perry, *Angew. Chem. Int. Ed*, 2008, 47, 709.
14. M. D. Torres, S. Semin, L. Razdolski, J. l. Xu, *Chem. Commun*, 2015, 51, 2855.
15. N. V. Krishna, V. K. Singh, D. Swain, S. V. Rao, L. Giribabu, *RCS Adv*, 2015, 5, 20810.
16. Z. H. Shi, Y. S. Zhou, L. J. Zhang, C. C. Mu, H. Z. Ren, D. Hassan, D. Yang, H. M. Asif, *RSC. Adv*, 2014, 4, 50277.
17. Z. H. Shi, Y. S. Zhou, L. J. Zhang, S. Hassan, N. N. Qu, *J. Phys. Chem. C*, 2014, 118, 6413.
18. Z. H. Wei, H. X. Li, Z. G. Ren, J. P. Lang, Y. Zhang, Z. R. Sun, *Dalton Trans*, 2009, 3425.
19. C. Zhang, Y. Cao, J. F. Zhang, S. C. Meng, T. Matsumoto, Y. L. Song, *Adv. Mater*, 2008, 20, 1870.
20. W. H. Zhang, Y. L. Song, Y. Zhang, J. P. Lang, *Cryst. Growth Des*, 2008, 8, 253.
21. H. H. Wu, Q. H. Gong, D. H. Olson , J. Li, *Chem. Rev*, 2012, 112, 836.
22. M. Y. Yoon, R. Srirambalaji and K. Kim, *Chem. Rev*., 2012 ,112, 1196.
23. J. R. Li, J. L. Sculley, H. C. Zhou, *Chem. Rev*, 2012, 112, 869.
24. L. E. Kreno, K, Leong, O, K, Farha, M. Allendorf, R. P. Van Duyne, J. T. Hupp, *Chem. Rev*, 2012, 112, 1105.
25. L. K, li, B. G. Chen, Y. L. Song, G. Li, H. W. Hou, Y. T. fan, L. W. Mi, *Inorg. Chim. Acta*, 2003, 344, 95.
26. H. W. Hou, X. R. Meng, Y. L. Song, Y. T. Fan, Y. Zhu, H. J. Lu, C. X. Chen, W. H. Shao, *Inorg. Chem*, 2002, 41, 4068.
27. W. Zhou, X. R. Meng, Y. N. Ding, W. Q. Li, H. W. Hou, Y. L. Song, Y. T. Fan, *J. Mol. Struct*, 2009, 937, 100.
28. H. W. Hou, Y. L. Song, Y. T. Fan, L. P. Zhang, C. X. Du, Y. Zhu, *Inorg. Chim. Acta*, 2001, 316, 140.
29. Y. Y. Niu, N. Zhang, Y. L. Song, H. W. Hou, Y. T, Fan, Z. Zhu, Inorg. *Chem. Commun*, 2005, 8, 495.
30. H. Xu, Y. L. Song, L. W. Mi, H. H. Wei, M. S. Tang, Y. L. Sang, Y. T. Fan, Y. Pan, *Dalton Trans*, 2006, 838.
31. H. W. Hou, Y. L. Wei, Y. T. Fan, C. X. Du, Y. Zhu, Y. L. Song, Y. Y. Niu, X. Q. Xin, *Inorg. Chim, Acta*, 2001, 319, 212.
32. H. W. Hou, Y. L. Wei, Y. L. Song, Y. Zhu, L. K. Li, Y. T. Fan, *J. Mater. Chem*, 2002, 12, 838.
33. H. W. Hou, Y. L. Wei, Y. L. Song, L. W. Mi, M. S. Tang, L. K. Li, Y. T. Fan, *Angew. Chem*, 2005, 117, 6221.
34. G. H. Wei, J. Yang, J. F. Ma, Y. Y. Liu, S. L. Li, L. P. Zhang, *Dalton Trans*, 2008, 3080.
35. Y. Qi, Y. X. Che, F. Luo, S. R. Batten, Y. Liu, J. M. Zhang, *Cryst. Growth Des*, 2008, 8, 1654.
36. J. Yang, J. F. Ma, Y. Y. Liu, J. C. Ma, S. R. Batten, *Cryst. Growth Des*, 2008, 8, 4383.
37. X. Z. Song, S. Y. Song, C. Qin, S. Q. Su, S. N. Zhao, M. Zhu, Z. M. Hao, H. J. Zhang, *Cryst. Growth Des*, 2012, 12, 253.
38. Z. M. Sun, J. G. Mao, Y. Q. Sun, H. Y. Zeng, A. Clearfield, *Inorg. Chem*, 2004, 43, 336.
39. Q. Y. Liu, D. Q. Yuan, L. Xu, *Cryst. Growth Des*, 2007, 7, 1832.
40. Gaussian 09, M. J. Frisch, G. W. Trucks, H. B. Schlegel, G. E. Scuseria, M. A. Robb, J. R. Cheeseman, G. Scalmani, V. Barone, B. Mennucci, G. A. Petersson, H. Nakatsuji, M.

Caricato, X. Li, H. P. Hratchian, A. F. Izmaylov, J. Bloino, G. Zheng, J. L. Sonnenberg, M. Hada, M. Ehara, K. Toyota, R. Fukuda, J. Hasegawa, M. Ishida, T. Nakajima, Y. Honda, O. Kitao, H. Nakai, T. Vreven, J. A. Montgomery, Jr, J. E. Peralta, F. Ogliaro, M. Bearpark, J. J. Heyd, E. Brothers, K. N. Kudin, V. N. Staroverov, R. Kobayashi, J. Normand, K. Raghavachari, A. Rendell, J. C. Burant, S. S. Iyengar, J. Tomasi, M. Cossi, N. Rega, J. M. Millam, M. Klene, J. E. Knox, J. B. Cross, V. Bakken, C. Adamo, J. Jaramillo, R. Gomperts, R. E. Stratmann, O. Yazyev, A. J. Austin, R. Cammi, C. Pomelli, J. W. Ochterski, R. L. Martin, K. Morokuma, V. G. Zakrzewski, G. A. Voth, P. Salvador, J. J. Dannenberg, S. Dapprich, A. D. Daniels, O. Farkas, J. B. Foresman, J. V. Ortiz, J. Cioslowski, and D. J. Fox, Gaussian, Inc., Wallingford CT, 2009.

41. G. M. Sheldrick, *Acta Cryst*, 2008, A64, 112.
42. Y. Y. Xu, Y. Y. Xing, X. Y. Duan, Y. Z. Li, H. Z. Zhu, Q. J. Meng, *CrystEngComm*, 2010, 12, 567.
43. G. H. Cui, J. R. Li, J. L. Tian, X. H. Bu, S. R. Batten, *Cryst. Growth Des*, 2005, 5, 1775.
44. S. L. Xiao, L. Liu, P. J. Ma, G. H. Cui, Z. *Anorg. Allg. Chem*, 2014, 640, 1484.
45. J. M. Hao, Y. N. Zhao, B. Y. Yu, K. Van. Hecke, G. H. Cui, *Transition. Met Chem*, 2014, 39, 741.
46. M. S. Bahae, A. A. Said, E. W. V. Stryland, *Opt. Lett*, 1989, 14, 955.
47. M. S. Bahae, A. A. Said, T. H. Wei, D. J. Hagan, E. W. V. Stryland, *IEEE J. Quantum Electron*, 1990, 26, 760.
48. H. Nakanishi, *Nonlinear Optics*, 1991, 1, 223.
49. T. Kobayashi, *IEICE Trans. Fundamental*, 1992, E75-A, 38.
50. G. D. Tang, S. S. Kou, Z. C. Zhang, T. T. Tang, L. F. Culnane, Y. Zhang, Y. L. Song, *Synth. Met*. 2013, 182, 60.
51. S. S. Kou, G. D. Tang, T. T. Tang, Y. Zhang, Y. L. Song, *Deys and Pigments*. 2014, 104, 102.
52. K. Li, G. D. Tang, S. S. Kou, L. F. Culnane, Y. Zhang, Y. L. Song, R. G. Li, C. M. Wei, *Spectrochim. Acta A*, 2011, 79, 137.
53. T. Lu, F. W Chen, *Acta Chim. Sinica*, 2011, 69, 2393.